Development and characterization of a gold nanoparticles glassy carbon modified electrode for dithiotreitol (DTT) detection suitable to be applied for determination of atmospheric particulate oxidative potential

Maria Pia Romano [a], Maria Giulia Lionetto [b], Annarosa Mangone [c], Anna Rita De Bartolomeo [b], Maria Elena Giordano [b], Daniele Contini [d], Maria Rachele Guascito [b, *]

[a] Dipartimento di Matematica e Fisica, Università del Salento, 73100, Lecce, Italy
[b] Dipartimento di Scienze e Tecnologie Biologiche e Ambientali, Università del Salento, 73100, Lecce, Italy
[c] Dipartimento di Chimica, Università degli Studi di Bari Aldo Moro, 70124, Bari, Italy
[d] Istituto di Scienze dell'Atmosfera e del Clima, ISAC-CNR, 73100, Lecce, Italy

HIGHLIGHTS

- Development of modified GC electrodes with electrodeposited gold nanoparticles.
- XPS and SEM/EDS characterization of the GC/AuNPs modified electrodes.
- Electrochemical characterization of the GC/AuNPs sensor to detect dithiotreitol (DTT).
- Electroanalytical performances of the sensor make it suitable to detect DTT in PM aqueous extracts.
- Electrochemical DTT assay as an alternative to classic spectrophotometric assay in OP determination.

GRAPHICAL ABSTRACT
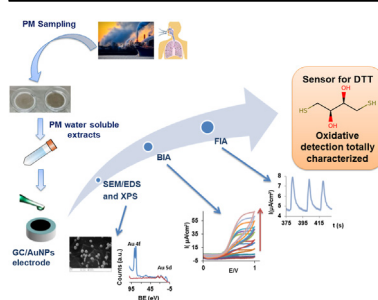
ARTICLE INFO

ABSTRACT

A gold nanostructured electrochemical sensor based on modified GC electrode for thiols' detection is described and characterized. This sensor is a suitable device for the measurement of the oxidative potential (OP) of the atmospheric particulate matter (PM), considered a global indicator of adverse health effects of PM, as an alternative to the classic spectrophotometric methods. The operating principle is the determination of the OP, through the measurement of the consumption of DTT content. The DTT-based chemical reactivity is indeed a quantitative acellular probe for assessment of the capacity of the atmospheric PM to catalyze reactive oxygen species generation which contributes to the induction of oxidative stress in living organisms and in turn to the outcome of adverse health effects. To make the sensors, glassy carbon electrodes, traditional (GC) and screen printed (SPE) electrodes, have been electrochemically modified with well-shaped rounded gold nanoparticles (AuNPs) by using a deposition method that allows obtaining a stable and efficient modified surface in a very simple and reproducible modality. The chemical and morphological characterization of the nano-hybrid material has been performed by X-ray photoelectron spectroscopy (XPS) and scanning electron microscopy coupled with electron dispersive spectroscopy analysis (SEM/EDS). The electrochemical properties have been evaluated by cyclic voltammetry (CV) and chrono-amperometry (CA) in phosphate buffer at neutral pH as requested in DTT

* Corresponding author.
  E-mail address: maria.rachele.guascito@unisalento.it (M.R. Guascito).

assay for OP measurements. The electroanalytical performances of the sensor in DTT detection are strongly encouraging showing low LODs (0.750 μM and 1.5 μM), high sensitivity (0.0622 μA cm^{-2} μM^{-1} and 0.0281 μA cm^{-2} μM^{-1}), wide linear and dynamic ranges extending over 2-4 orders of magnitude and high selectivity. FIA preliminary results obtained on measuring the DTT rate consumption in six PM aqueous extracts samples showed a good correlation with measurements obtained in parallel on the same set of samples by using the classic spectrophotometric method based on the Ellman's reactive use. These results confirm the high selectivity of the method and its suitability for application to be applied in PM oxidative potential measurements.

1. Introduction

The thiols are important molecules involved in biological and environmental processes. The presence of thiols in living systems is critical for the maintenance of cellular redox potentials and protein thiol-disulfide ratios, as well as for the protection of cells from reactive oxygen species [1].

The role of reduced endogenous thiols (RSH) is essential in maintaining the cellular redox state, therefore their concentration and bioavailability are very important in the balance and prevention of oxidative stress associated with various diseases (i.e. cancer, atherosclerosis, diabetes mellitus, and so on) [2,3]. RSH such as homocysteine (HCys), glutathione (GSH), acetylcysteine (ACys) and cysteine (Cys) are the most common plasma low-molecular-mass aminothiols involved in important functions in metabolism and homeostasis [4]. The changes in their content and metabolism can affect important intracellular pathways [5]. Detection of these RSHs is typically made directly thanks to their relatively high reactivity, thus, the most common methodologies for thiols quantification involve the determination of free thiols concentration [6]. To date, one of the methods most widely used for the detection of thiols in the biological samples is the classical Ellman's spectrophotometric test introduced by Ellman in 1959 [7]. Many different other analytical techniques have been developed including Capillary Electrophoresis (CE), High-Performance Liquid Chromatography (HPLC), Flow Injection Analysis (FIA), and Fluorescence [8]. Recently, Konno [9] in 2020 described the thiol functionality and intramolecular disulfide bond formation of peptides using the α-Keggin type polyoxometalate molybdenum−oxygen cluster.

In addition to these methods, the electroanalytical techniques, often coupled as a detector with separative techniques are well represented in the thiols detection literature [10–13], and references therein. The electrochemical methodologies include direct thiols oxidation, the simplest approach to their analytic measurement at bare solid substrates [10]. However, large overpotentials are required before a sufficient sensitivity can be attained, as required in the complex matrices analysis. A problem with direct amperometric detection of thiols at noble metal electrodes (i.e. Pt and Au) is the passivation. The mechanism of detection involves adsorption of the analytes to the electrode via the sulfur atom and subsequent oxidation giving an analytical signal. Unfortunately, the surface oxide formation which catalyzes the detection also passivates the electrode to further thiols adsorption [10]. Nevertheless, several materials have been investigated as for example glassy carbon (GC) [14,15], carbon [16], graphite and platinum [17], gold [18], and silver [19]. To overcome these problems, transition metal complexes modified electrodes have been proposed as electrocatalytic agents acting as redox mediators to lower thiols oxidation overpotential. Between these metal complex modifiers the cobalt phthalocyanines (CoPCs), firstly introduced from Baldwin group's [20,21], represent to date one of the most employed composts class

to direct electro-oxidative detection of thiols [22–26]. The organic thiols have been detected also via voltammetric protocols by adapting the Ellman's test [27]. These methods are based on indirect detection of thiol compounds by electrochemically measuring the nitro groups present on both DTNB reagent and the resulting TNBA reaction product. The use of the reducing potentials allows to avoid passivation and improve the selectivity decreasing interference effects.

Among the thiols, DTT, or Cleland's reagent [28], is commonly used as a protective reagent to reduce disulfide bridges in proteins and prevent dimerization of sulfur atoms of thiolated DNA for its low redox potential (-330 mV at pH = 7) since the 1960s [29]. The areas of DTT application include biochemical preparations of protein thiols, chemical peptide synthesis and studies of protein chemistry. Alongside these DTT applications, a work of Kumagai et al. [30] has demonstrated that the redox-active quinones (i.e. 9,10-phenanthraquinone) can effectively catalyze the transfer of electrons from dithiothreitol (DTT) to oxygen, generating superoxide. The authors demonstrated that quinones in diesel exhaust particles promote reactive oxygen superoxide (ROS) generation in biological systems. Starting from this pioneering paper, Cho et al. [31] have proposed the DTT reactivity as a quantitative acellular probe for the assessment of the capacity of the atmospheric particulate matter (PM) to catalyze ROS generation, responsible for the oxidative stress induced in organisms and heavily affecting human health [32–34]. The concern about the exposure to PM and the possible related risks for human health has considerably grown in the last several years. However, to date, the exact mechanism by which the PM causes oxidative stress, is not totally clear. The most probable cause is the generation of unstable ROS (i.e. peroxides, superoxide, hydroxyl radical, and singlet oxygen) [24], formed by the incomplete reduction of molecular oxygen attributed to PM chemical composition with particular attention to aromatic compounds as well as transition metals (i.e. Fe, V, Cr, Mn, Co, Ni, Cu, Zn, and Ti) [23,35]. In this contest, many efforts have been done to develop analytical techniques with the purpose of better clarifing and understanding these harmful effects of PM on human health. The spectrophotometric DTT assay, as proposed by Cho et al. [31] and its successive modifications, is one of the most employed chemical methods to quantitatively assess the OP associated with the PM [36,37], commonly used as cells-free measure of the oxidative potential of particles [38–40].

In this assay, reduced DTT in presence of ROS, generated by PM, is oxidized to its disulfide. After the reaction, the remaining reduced DTT reacts quantitatively with Ellman's reagent 5,5′-dithio-bis-(2-nitrobenzoic acid) (DNTB) to form 2-nitro-5-thiobenzoic acid (TNB). The rate of DTT consumption measured at different reaction times is proportional to the oxidative activity of the PM sample. Therefore, the DTT-based chemical assay has been introduced to quantitatively measure the oxidative potential of PM, defined as a measure of the capacity of PM to oxidize target

molecules, by generating ROS in environments without living cells. Operatively, the OP is defined by the DTT consumption rate normalized by PM collected mass or sampling volume [41]. The high diffusion of the DTT test, compared to other reported cells-free assays [38] is attributable to its low-cost, easy-to-operate, high repeatability and because it can be easily conducted on a laboratory bench scale, providing a fast output under an easily-controlled environment [38]. In this context, due to the pressing need to quickly obtain information on the oxidizing properties of PM to assess air quality, efforts have been made to automate the spectrophotometric DTT assay to operate in flow modality [42]. The major encountered problems regard the use of different reagents needed to finalize the test. These obstacles can be overcome by measuring directly the DTT rate depletion in PM extract by electrochemical detection.

Despite some encouraging results and advantages in using direct DTT electrochemical detection, electrochemical assays are poorly represented in current literature: only a few researchers have proposed to detect the ROS in PM by measuring the rate depletion of DTT as far as cytochrome (cyt-c) by adopting electrochemical measurements as an alternative to the traditionally spectrophotometric methods based on the Ellman's reactive use. Furthermore, Sameenoi [23,43], Koehler [24] and, most recently, Berg [26] adapted cobalt(II) phthalocyanines (CoPCs)-modified carbon paste electrodes (CPEs), as introduced by Halbert and Baldwin [21], and successive modifications, to realise electrochemical automated sensing devices, in FIA and microfluidic measurements. In particular, Berg [26] introduced a semi-automated DTT assay using a traditional HPLC technique combined with both UV/vis absorbance and electrochemical detection that has shown comparable accuracy and sensitivity to manual approaches. However, although the extensive use and new opportunity given from the nanotechnology in the development of electrochemical sensors is documented for thiols detection [44], particularly for GSH detection as highlighted in a recent paper [45] and dedicated reviews [11–13], to the best of our knowledge no electrochemical sensors based on nanostructured materials have been specifically reported to detect DTT, in atmospheric aerosol OP monitoring, as an alternative to CoPCs based modifiers.

At the state of the art, different methods of AuNPs electrodeposition have been reported to obtain modified GC electrodes, with high electro catalytic properties in different application fields [46–49]. Based on these previous works, in this study we have proposed an electrochemical preparation method to obtain a gold nano-particles modified electrode (GC/AuNPs), suitable to be used as an amperometric sensor for the electroanalytical detection of DTT at pH 7.4, in alternative to the CoPCs based modifiers. This hybrid material has been chemically and morphologically characterized, respectively, by XPS and SEM/EDS analysis. The electrochemical properties of GC/AuNPs chemically modified electrodes have been characterized by CV in phosphate buffer in batch analysis in the presence and absence of DTT analyte, respectively. The electroanalytical performances of the new sensor have been reported in terms of LODs, linear and dynamic ranges, sensitivity and selectivity. The interference studies of real PM aqueous extracts in the electrochemical response to DTT have been reported to be very low or absent. Tests in FIA analysis were done to assess the DTT consuming rate in different PM aqueous extracts and validated with respect the classic spectrophotometric method.

2. Experimental details

2.1. Materials

The following analytical grade chemicals and materials have been used as received: Gold (III) chloride trihydrate 99.9+% $(AuCl_3(H_2O)_3)$ from Sigma Aldrich; DL-Dithiothreitol (DTT) from VWR Chemicals; 9,10−phenanthraquinone (PQN) from Alfa Aesar; MicroPolish Powder (1.0 and 0.3 μm) from CH instrument. All the aqueous solutions were prepared using Millipore water (Millipore Milli-Q 18.2 MΩcm). For the DTT aqueous solution 6 mM, 9.258 mg of DTT have been dissolved in 10 mL of phosphate buffer (pH = 7.4; I = 0.2), which was prepared from KH_2PO_4 e Na_2HPO_4 from Fluka.

2.2. PM_{10} sampling and extraction from filters

Nine daily PM_{10} samples were collected, starting at midnight, on quartz filters (Whatman, 47 mm in diameter) at low volume (2.3 m^3/h) using a sequential dual channel automatic sampler (SWAM, Fai Instruments srl) equipped with ß-ray attenuation detection of PM concentration [50]. PM_{10} samples were taken at the Environmental-Climate-Observatory (ECO) of Lecce, regional station of the GAW-WMO network that is characterised as an urban background station [51]. Aqueous PM_{10} extracts were obtained in 15 mL of potassium phosphate buffer 0.1 M, using ultra-sonication at room temperature for 30 min, to make interference studies and DTT rate consumption measurements in PM extracts to determine related OPs. More details on the experimental approaches are given in the supporting material and summarized in Table S1.

2.3. Equipment

The electrochemical experiments in batch and in flow have been carried out by using a DropSens electrochemical workstation (DropSens ST40010140) controlled by computer. In batch experiments a conventional three-electrode cell has been used with a Pt wire as counter electrode and an Ag/AgCl as reference electrode. The working electrodes were: bare Au (0.0314 cm^2), bare GC (0.0706 cm^2), and bare GC modified with gold nano-particles (GC/AuNPs). All voltammetric and amperometric experiments have been performed in a phosphate buffer solution (pH 7.4). N$_2$ had been bubbling for 15 min before the beginning of the batch experiments to minimize possible environmental oxygen interference (i.e. DTT degradation), in the course of the measurements. The nitrogen atmosphere had been preserved in the cell throughout all the measurements. Concerning the flow experiments, the experimental details are available on the supporting file with the related Scheme S1.

The repeatability of the sensors at different DTT concentration levels was obtained in batch analysis by averaging results obtained in three independent experiments on the same electrode in the same concentration range. The same procedure was repeated at least on three distinguished GC/AuNPs electrodes to test the reproducibility. In FIA experiments repeatability, each DTT solution was injected at least three times for two distinct successive experiments (in total six replicate for run) on the same SPE_GC/AuNPs, injected volume 65 μL. The same procedure was repeated at least on three distinguished SPE_GC/AuNPs to test the sensors' reproducibility. Both repeatability and reproducibility were expressed in terms of Relative Standard Deviation (RSD, bar errors as appropriate in figures) and the RSD of the calibration slope (RSD$_{slope}$).

Plates made of Glassy Carbon SIGRADURG (15 × 10mm^2, thickness 0.5 mm) bare and modified, have been utilized for the XPS and SEM/EDS characterization.

2.4. Preparation of Au nanoparticles modified electrodes

All bare working electrodes (GC and Au) were opportunely treated to obtain a clean and activated surface before

M.P. Romano, M.G. Lionetto, A. Mangone et al.

electrochemical characterization and/or chemical modifications. The surface of bare electrodes (GC and Au) was mechanically lapped with MicroPolish Powders (1.0 and 0.3 μm). Then, both electrodes GC and Au were chemically etched, for 20 min, with a drop of sulfuric acid and a drop of hydrochloric acid, respectively, and thoroughly washed and sonicated for 10 min in deionised water. After this mechanical and chemical treatment, the electrodes were cycled by CV in the potential range of −1.000 V to +1.500 V, in phosphate buffer solution (pH 7.4), until a steady-state conditions were reached (almost 20 cycles), in order to obtain reproducible/activated surfaces.

Modified electrodes were prepared by direct drop-casting $AuCl_3$ (137 μM) aqueous solution on a bare GC electrode, previously prepared as above described. The solution after use was maintained at 4 °C for some weeks. Concerning the direct drop casting: 15 μL of solution were casted in three different additions of 5 μL each one, the second and the third 1 h after the previous ones, in order to spontaneously dry the surface. Subsequently, the Au electrodeposition had been conducted by chronoamperometry at the applied potential of −900 mV vs Ag/AgCl for t = 200s in not stirred phosphate buffer. The typical CA was reported in Fig. S1 (a). After the GC modified electrode was cycled in clean phosphate buffer solution (pH 7.4) between −1000 mV and 1500 mV until the steady-state condition (typically 20 cycles) was reached (last cycle is reported in Fig. S1 (b). Tests on electrodes prepared by casting 5 μL and 25 μL of $AuCl_3$ have been also done. Similarly, the SPE_GC/AuNPs modified electrodes preparation for the FIA experiments had followed the same steps.

2.5. Spectroscopic characterization by XPS and SEM-EDS analysis

The XPS spectra were recorded using an AXIS ULTRA DLD (Kratos Analytical spectrometer, Kyoto, Japan) instrument, equipped with a monochromatic anode (Al Kα) source that operate at 150 W. Survey spectra were collected at 1 eV and detailed spectra of C1s, O1s, Au5d, C (A) and valence band (VB) regions at 0.1 eV step intervals, in Fixed Analyser Transmission (FAT) mode at $E_0 = 20$ eV. A hybrid lens mode was used for all measurements with analysis area of about 700 μm × 300 μm.

The XPS spectra were collected on GC slides samples (1cmx1.5cmx0.2 cm), cleaned and electrochemically activated as reported for classical GC electrodes, and on GC slides AuNPs modified (see 2.2 paragraph), for comparison. No X-ray induced decomposition of samples was observed during XPS data acquisition, as manifested by changing peak areas or shifting of positions. During the data acquisition, a careful charging effect correction has been made by using the charge neutralization with a filament current, filament bias voltage, and charge balance voltage of 2.0 A, 1.3 V and 3.6 V. All the experimental BE values were correct by setting the binding energy of C1s hydrocarbon photo-peak at 285.0 eV used as an internal standard [52]. Data analysis of high-resolution spectra was performed using the fitting program New Googly [53]. This program allows satellites and background correction. Peaks assignment has been done by comparing the binding energy (uncertainty of ±0.1 eV) to that reported in the literature and in the standard reference database of the National Institute of Standard and Technology (NIST X-ray Photoelectron Spectroscopy Database.).

The SEM investigations, on GC and GC AuNPS modified slides, prepared as before, were performed with a LEO EVO-50XVP (Zeiss, Cambridge, Cambridgeshire, UK) coupled with an X-max (80 mm^2) Silicon drift Oxford detector (Oxford Instruments, High Wycombe, Buckinghamshire, UK) equipped with a Super Atmosphere Thin Window ©.

3. Results and discussion

3.1. GC/AuNPs morphological and chemical characterization

Typical SEM images of AuNPs population as synthesized on GC surface are shown in Fig. 1 (b), (c) and (d). SEM observations clearly show that as synthesized NPs were randomly distributed on the GC substrate surface layer and they had typical spherical shape with smooth surfaces and uniform diameters on average of 250 nm. These spheres tends to be aggregated in some regions of the surface. The EDS data have been acquired respectively on the corresponding AuNPs and GC selected area spot regions (data not shown). As expected, the Au EDS signals are detected only on spot focused on aggregated spheres present on GC/AuNPs. The absence of chlorine EDS signals confirms that the deposited gold phase was pure gold, thus excluding the presence of $AuCl_3$ residual salt coming from the casted solution. The SEM image of bare GC substrate is also shown for comparison (Fig. 1 (a)). The relevant EDS analysis acquired on GC bare does not show Au signals, as expected.

XPS spectra were acquired to chemically characterize the surface of GC/AuNPs modified electrodes. For comparison, results relevant to bare GC electrodes have been also analyzed. In Fig. 1 (e), the wide scan acquired onto GC (red trace) and GC/AuNPs modified electrodes (blue trace), is reported. As expected the C1s and O1s peak signals are the most intense on both sample typologies, moreover the Au 4f and Au 5d (detailed in Fig. 1 (f)) peak signals related to gold nanoparticles are present only on GC/AuNPs. Fig. S2 shows the typical example of fit of the C1s region of GC slide. Analogously, the C1s peak related to GC AuNPs modified (Fig. 1 (g)), was fitted by using the same five components as for GC, however it was necessary to add a new component at 283.1 ± 0.1 eV to take into account the asymmetry now present at lower binding energy (Fig. 1 (h)). Au4f peak present on GC AuNPs, has been fitted by using two spin−orbit split doublets (Fig. 1 (i)). The first doublet (Au4f7/2 and Au4f5/2) is related to the most intense Au component that shows well separated spin-orbit splitting peaks, at 83.9 ± 0.1 s eV and 87.6 ± 0.1 eV respectively, is assigned to Au(0). The peak fit parameters have been obtained by gold slide signal used as standard reference (Fig. 1 (l)). However, near the Au (0) bulk component, a different form of gold is also observed (peak pair Au4f7/2 at 84.9 ± 0.1 eV and Au4f5/2 at 88.4 ± 0.1 eV), always associated to the presence of carbide C1s peak signal at 283.1 ± 0.1 eV [54]. Accordingly, this Au peak component is attributed to Au(I), likely originated from a surface gold carbide species [55]. This component was totally absent, on pure gold sample as obtained before and after sputtering with Ar ions beam. The atomic ratio (At %) between gold and C, averaged on 10 different analyzed area spots (700 μm × 300 μm), is almost 0.8 ± 0.2%, confirming that the gold is not deposited in a 2D mono/multilayer film structure according to SEM images.

3.2. Electrochemical characterization of GC/AuNPs modified electrodes

The electrochemical characterization of the GC/AuNPs modified electrodes was obtained by CV in phosphate buffer (pH = 7.4) at 50 mVs^{-1} between −1000 mV and +1500 mV and a comparison has been made between the bare GC and the Au electrodes. The results and related comments are reported in the supporting (Fig. S3). The GC/AuNPs modified electrodes behaviors suggest that the electrodeposited gold nanostructure has different electrochemical properties compared to the ones of gold bulk and provides peculiar properties to GC modified electrodes, probably thanks to a synergic effect between AuNPs and glassy carbon substrate interactions.
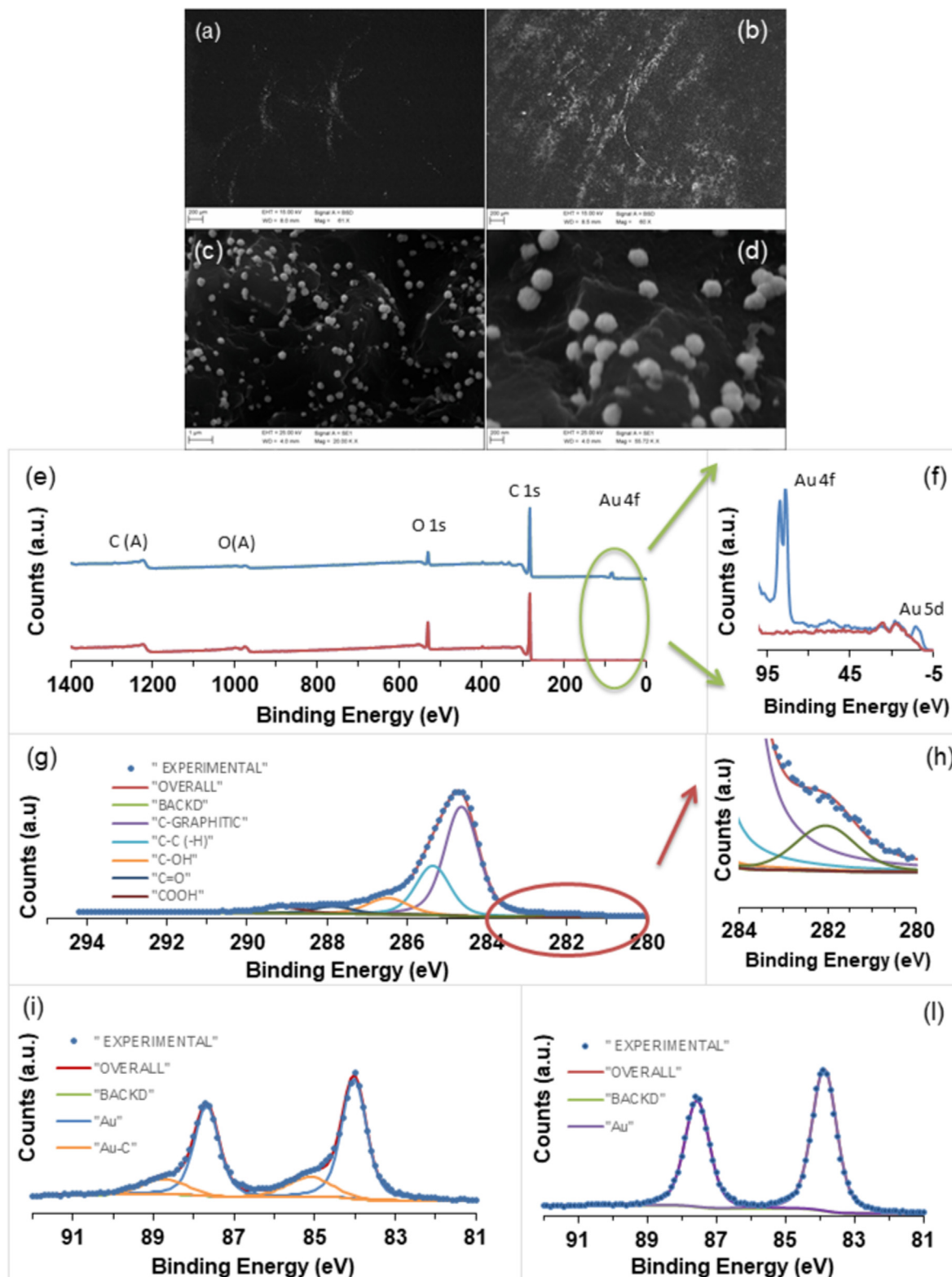
Fig. 1. (a) SEM image of GC bare surface; (b) (c) and (d) SEM images of GC/AuNPs modified electrode; (e) XPS survey spectra on GC (red line) and GC/AuNPs (blue line); (f) Details of Au4f and Au5d regions. (g) Curve fit of C1s HR peak region on GCAuNPs; (h) Detail of C1s curve fit. (i) Curve fit of Au4f HR peak region on GC AuNPs. (l) Curve fit of Au4f HR peak region on sputtered Au slide. (For interpretation of the references to colour in this figure legend, the reader is referred to the Web version of this article.)

M.P. Romano, M.G. Lionetto, A. Mangone et al.

3.3. Electrochemical characterization of GC/AuNPs sensor in DTT detection

The GC/AuNPs reactivity towards the DTT electro-oxidation in phosphate buffer has been studied in order to demonstrate that the electrochemical properties of the deposited gold nanoparticles can also improve the well known GC electroactive properties. The results confirmed that both the GC and GC/AuNPs electrodes show a reactivity towards the DTT electro-oxidation when they are studied in the potential range between 0.000 mV and +1500 mV. In Fig. 2 (a) the increment of the anodic currents after DTT 500 μM addition (red trace), is evident on GC bare electrode. A peak current in oxidation at Epa = +1210 mV is observed, not coupled with a peak in reduction. This is in accord whit a total irreversible process, as already reported at neutral pH on GC electrodes, that has been associated to the oxidation of the sulfhydryl groups involving two electrons [15].

Similar behaviour have been likewise reported on GC/AuNPs modified electrodes (Fig. 2 (b)). Also in this case, after DTT 500 μM addition there is an evident irreversible peak in the oxidation at Epa = +1210 mV, according to the data obtained on GC bare electrode. However, the anodic peak current, obtained after subtracting the CV baseline recorded in absence of DTT for both the electrodes respectively (Fig. 2 (c)), shows a net increment for GC/AuNPs (yellow trace) if compared to GC bare electrode (blue trace). The anodic current peak measured is almost 261 μAcm^{-2} vs 171μAcm^{-2} on GC, with an increment of 152%. On both electrodes, the process of DTT

oxidation is catalytic considering that the current in the reverse scan is still anodic and the related decrement in current could be attributed to the electrodic surface poisoning by the adsorbed products of DTT electro-oxidation. However, the active surface of the modified electrode to respect DTT oxidation increases compared to the bare GC in presence of gold NPs. In addition, the on-set for the DTT oxidation on GC/AuNPs is shifted to a more negative potential: +300 mV vs +900 mV on the GC bare electrodes. This increment of the anodic current, which is being observed at one potential lower than the ones typical of the anodic peak starting, and which lasts until the constant value in the potential range +500 mV and +800 mV is reached, looks like an anodic pre-wave [56,57] associated to the process as schematized in (I) and already reported on gold nanostructured electrodes for cysteine oxidation [44]. The gold nanoparticles phase promoting the spontaneous adsorption of DTT with a strong gold−thiolate bonds formation (RS-Au) [58,59], helps the lowering of the large oxidative overpotentials required to oxidize sulfur on GC [12] and Au [56] bare electrodes. Instead, anodic peak at higher potentials, can be than attributed to the direct quantitative oxidation of thiol-groups on AuNPs and GC activated sites, to form sulfonic acid (process II, [56]) and sulfenic acid (process III, [15]), respectively. It's interesting that the total absence of gold oxide reduction peak confirms that the process II does not involve the formation of a stable gold oxide species.

$$R-S-H + Au(NPs) - e^- = R-S-AuNPs + H^+ \quad \text{(pre-wave, I)}$$
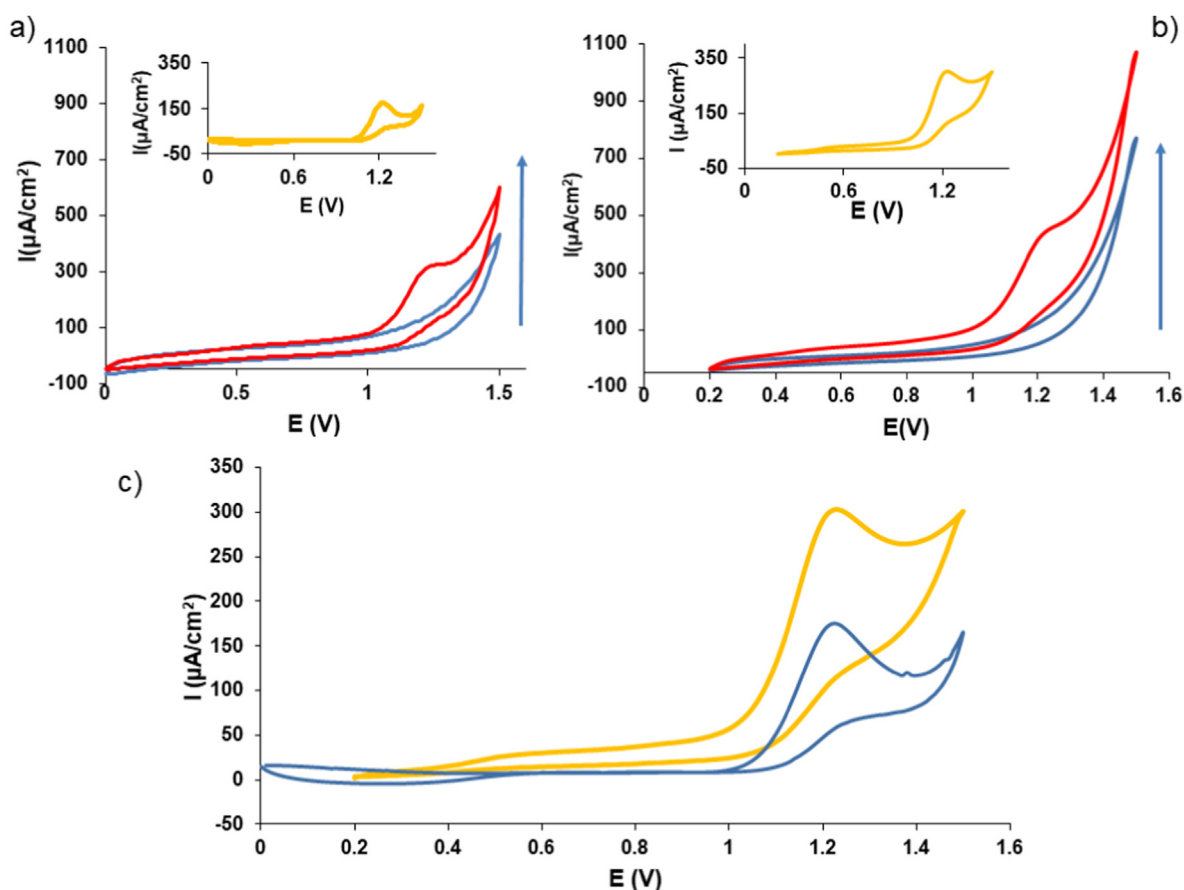
Fig. 2. (a) CVs recorded on GC electrode bare in absence (blue trace) and presence of DTT 500 μM (red trace). Inset: curve difference between CVs recorded in presence of DTT 500 μM and related base line. (b) CVs recorded on GC/AuNPs electrode in absence (blue trace) and presence of DTT 500 μM (red trace). Inset: curve difference between CV recorded in presence of DTT 500 μM and related base line. (c) Direct comparison between curves differences (GC, blue trace; GC/AuNPs, yellow trace). Scan rate 50 mVs^{-1}. (For interpretation of the references to colour in this figure legend, the reader is referred to the Web version of this article.)

M.P. Romano, M.G. Lionetto, A. Mangone et al.

$R-S\text{-}AuNPs + 3H_2O - 5e^- = R-SO_3^- + 6H^+$ (anodic peak, II)

$R\text{-}S\text{-}H$ (GC) $- 2e^- + H_2O = R\text{-}S\text{-}OH + 2H^+$ (anodic peak, III)
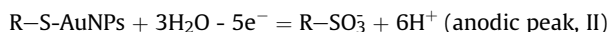
A similar behaviour suggests the possibility to make DTT detection on GC/AuNPs at much lower potentials than those on bare GC electrode and bare Au, between +500 and + 800 mV, being suitable to reduce interferences in real sample analysis.

The progressive addition of DTT in CV experiments, from the initial concentration of 19.6 μM until the final concentration of 500.0 μM and 783.0 μM, has been performed on the bare GC and on the GC/AuNPs electrodes, respectively. In Fig. 3 (a) and (b), CV curves obtained in presence of different DTT concentrations after subtracting the related base-line, in absence of DTT, were shown for both the electrodes. Inset reports the relevant calibration curves. On both electrodes, the catalytic peak currents (Ip) in oxidation were found to increase linearly in the DTT concentration ranging between 19.6 and 783 μM on GC/AuNPs and 19.6 and 500 μM on GC, with a determination coefficient of 0.996 and 0.997, as obtained by the regression analysis carried out with the following Eq. (1) on bare GC and Eq. (2) on GC/AuNPs electrodes, respectively.

$$Ip_{CG} (\mu Acm^{-2}) = 0.360 \, (\mu A \, cm^{-2} \, \mu M^{-1})C_{DTT}(\mu M) - 4.748 \, (\mu Acm^{-2}) \quad (1)$$

$$Ip_{CG/AuNPs} (\mu Acm^{-2}) = 0.443 \, (\mu A \, cm^{-2} \, \mu M^{-1})C_{DTT}(\mu M) + 49.747 \, (\mu Acm^{-2}) \quad (2)$$

A sensitivity of 0.443 $\mu Acm^{-2}\mu M^{-1}$ on GC/AuNPs, and 0.360 $\mu Acm^{-2}\mu M^{-1}$ on GC was obtained respectively. The difference between the Ip vs C_{DTT} curves intercept values in average is of 45 μAcm^{-2}. Both these increments, in current intensities and intercept, represent the contribution to the DTT overall oxidation process relevant to the activated RS-AuNPs formed at lower potentials on GC/AuNPs and not present on bare GC. The electro-catalytic DTT oxidative process (I), starting at +300 mV on GC/AuNPs electrodes, is confirmed from the rise of the current with DTT concentrations increment (Fig. 3 b). To study this process, the electrochemical oxidation of DTT on GC/AuNPs electrode was done in the potential range between 0.000 mV and +1000 mV in the DTT concentration range between 19.6 and 880 μM (Fig. 3 (c)). The shape of all CV curves are wave-like anodic currents and the current measured at the plateau (limit current, i_L), not-potential dependent, increased linearly with DTT concentration, with a determination coefficient of 0.996, as obtained by the regression analysis carried out with the following Eq. (3).

$$I_{LCG/AuNPs} (\mu Acm^{-2}) = 0.0781(\mu A \, cm^{-2}\mu M^{-1})C_{DTT} (\mu M) - 3.161 (\mu Acm^{-2}) \quad (3)$$

The analysis in this potential range shows a sensitivity of the method of 0.0781 $\mu A \, cm^{-2}\mu M^{-1}$.

The correlation between current and scan rate has been also studied between 2 mVs^{-1} and 800 mVs^{-1} (Fig. 4 (a)), in the potential range between -100 mV and $+1500$ mV, DTT 460 μM. The
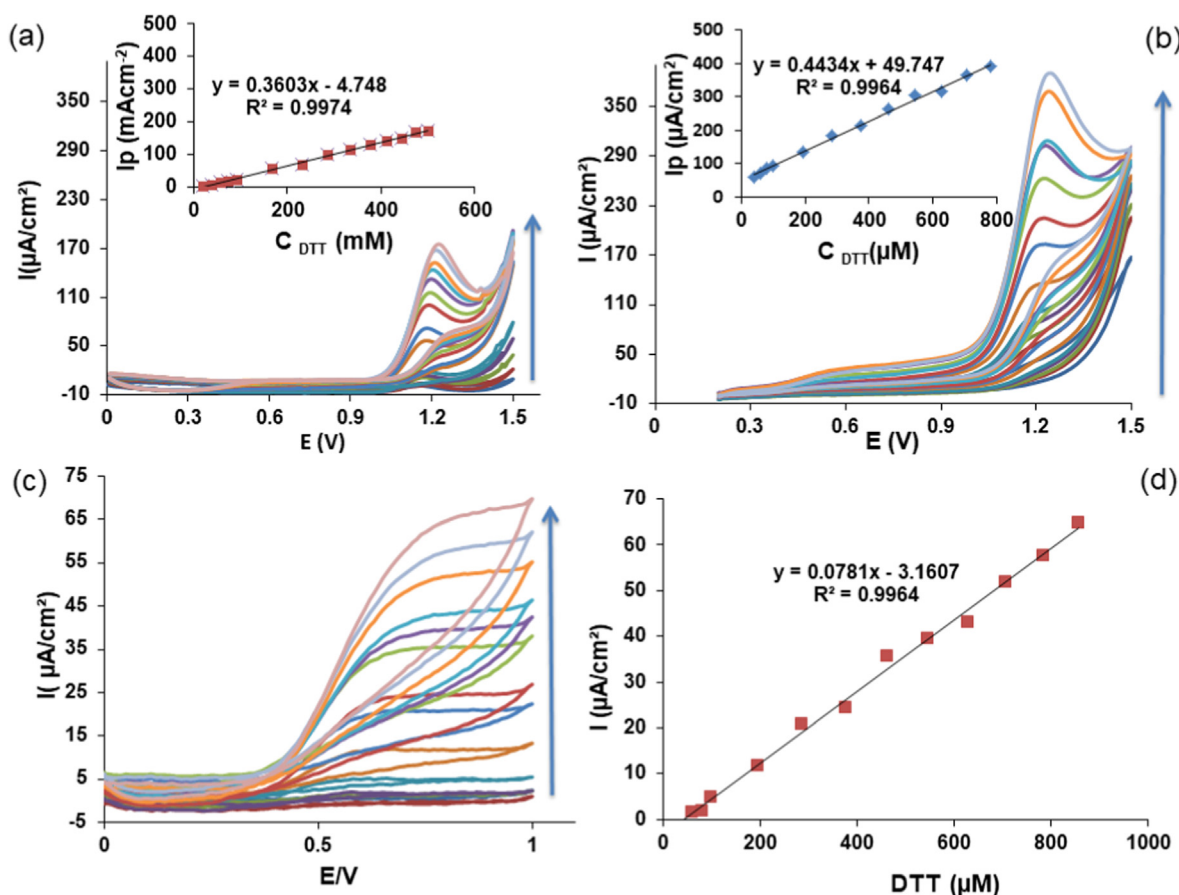
Fig. 3. (a) CVs recorded on bare GC electrode at different DTT concentrations between 19.6 μM and 500 μM, potential range between 0.000 mV and +1500 mV; Inset: plot of the anodic peak current Ip$_{aGC}$ in function of DTT concentrations; (b) CVs recorded on bare GC/AuNPs modified electrode between 19.6 μM and 784 μM, potential range +200 mV and 1500 mV; Inset: plot of the anodic peak current Ip$_{aGC/AuNPs}$ in function of DTT concentrations. (c) CVs recorded on bare GC/AuNPs modified electrode between 19.6 μM and 880.0 μM, potential range 0.000 mV and 1000 mV. (d) Plot of anodic current I$_{LGC/AuNPs}$ in function of DTT concentrations, measured at +800 mV. Scan rate 50 mVs^{-1}.

reported CV curves refer to the 3° cycle in steady-state condition. As expected, for a total irreversible process, by increasing the scan rate an anodic shift is observed for the anodic potential peak (Ep). In particular, a positive shift of +200 mV is observed when the scan rate goes from 2 mVs^{-1} (Epa = +1180 mV) to 800 mVs^{-1} (Epa = +1380 mV). A linear dependence of Ipa vs v$^{1/2}$ is observed (Eq. (4), R^2 = 0.997), confirming that the process is diffusion controlled. In the pre-wave region, I$_L$ measured at +600 mV, increased linearly with v (Eq. (5), R^2 = 0.991). This behaviour is in accord with a surface controlled process as expected in the hypothesis that the electrochemical process involves adsorbed electroactive species (i.e. AuNPs and RS-AuNPs adsorbed) according to Refs. [44,60].

$$Ip_{CG/AuNPs}\,(\mu Acm^{-2}) = 35.766[\,(\mu A\,cm^{-2})/\,(mVs^{-1})^{1/2}\,]\,v^{1/2}\,[\,(mVs^{-1})^{1/2}\,] + 97.268(\mu Acm^{-2}) \tag{4}$$

$$I_{LCG/AuNPs}\,(\mu Acm^{-2}) = 0.278[\,(\mu A\,cm^{-2})/(mVs^{-1})]\,v[\,(mVs^{-1})] + 18.487(\mu Acm^{-2}) \tag{5}$$

Based on these results, process (I) proceeds in a catalytic scheme where the adsorbed DTT on AuNPs islands reacts chemically with Au(I)NPs electrochemically formed at moderate potentials (between +300 mV and +800 mV) to regenerate Au(0)NPs starting material to form oxidized DTT (i.e. disulfide) [10]. Probably, initially the Au(0)NPs are electrochemically oxidized to Au(I)NPs, followed by the chemical oxidation of DTT as it regenerates Au(0)NPs form. Subsequently, at most anodic potentials, the catalytic reaction scheme could involve both the electrochemical oxidation to form sulfonic acid at AuNPs over-activated sites as far as sulfenic acid at

GC active sites (process II and III). Then, at moderate potential, the rate determining step is the DTT-AuNPs adsorption that involves surface confined Au(I)/Au(0)NPs electrocatalytic species, while at higher potentials, where a massive oxidation can be observed, the rate determining step is the DTT diffusion. It has to be highlighted that the current density signals don't saturate at the studied DTT concentration ranges in both potential regions. In addition, no stable gold oxidized species can be observed as observed on bare gold.

3.4. Chrono-amperometric DTT detection on GC/AuNPs modified electrode in batch analysis

The chrono-amperometric detection of DTT was tested in the concentration range (750 nM-1.150 mM) which includes the range useful for spectrophotometric DTT detection assay in oxidative potential measurement of aqueous samples of environmental origin, as aqueous extracts of particulate matter soluble fraction. DTT amperometric detection was done at +600 mV in batch condition under controlled stirring and in N$_2$ saturated atmosphere. This value has been selected by performing potentiodynamic measure at DTT concentration of 200 μM in batch condition at different applied potentials between +200 mV and +800 mV (Fig. S4).

Fig. 5 (a) (red trace) shows the behaviour of the modified electrode, at +600 mV, in comparison with GC bare electrodes (green trace) to test the activity of GC/AuNPs towards DTT electro-oxidation in the concentration range (750 nM - 1.150 mM). The amperometric detection experiments confirm that gold nanoparticles positively influence the behaviour of the sensor,
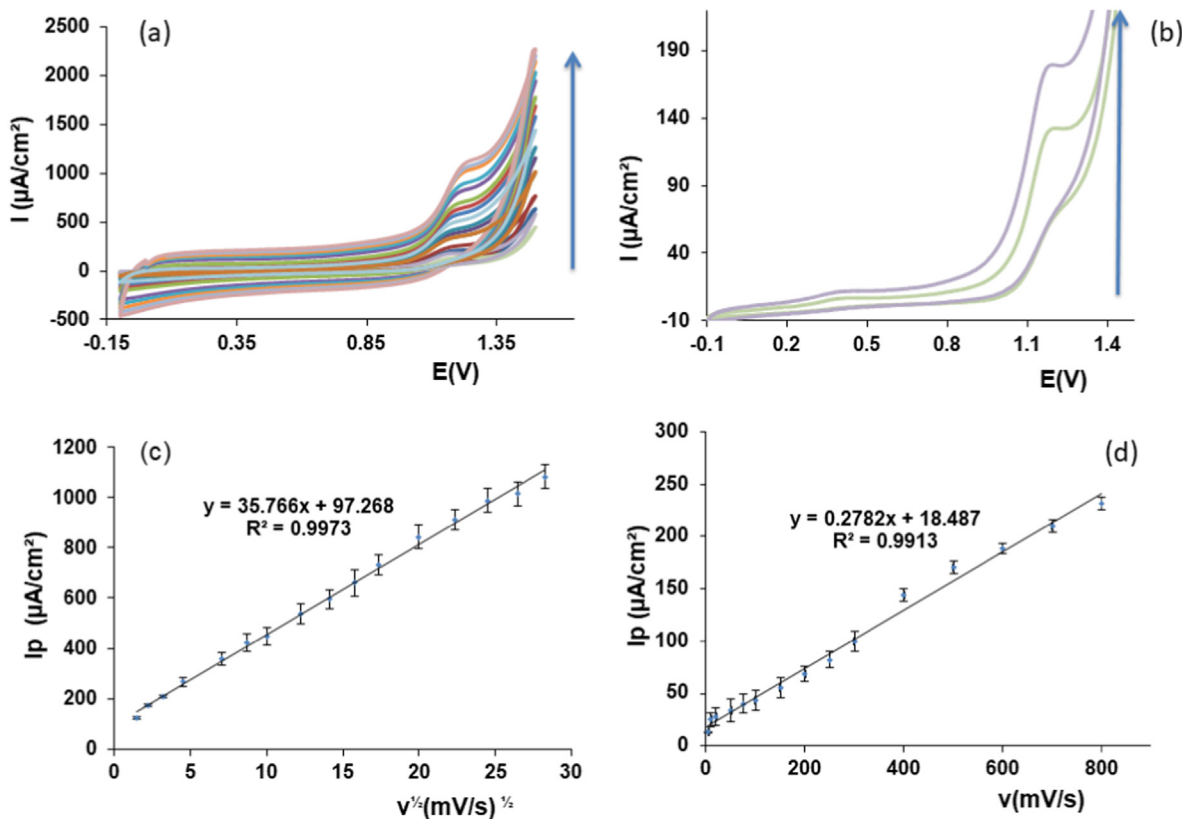
Fig. 4. (a) CVs recorded on GC/AuNPs electrode at different scan rate between 2 and 800 mV/s, potential range −100 mV and +1500 mV, DTT concentration 460 μM. (b) CVs detail at 2 and 5 mVs^{-1}, respectively. (c) Plot of the anodic peak current Ip$_{aGC/AuNPs}$ vs v$^{1/2}$; (d) Plot of the anodic limit current I$_{L\ GC/AuNPs}$ measured at +600 mV vs v. Error bars represent one standard deviation about the mean (n = 3).
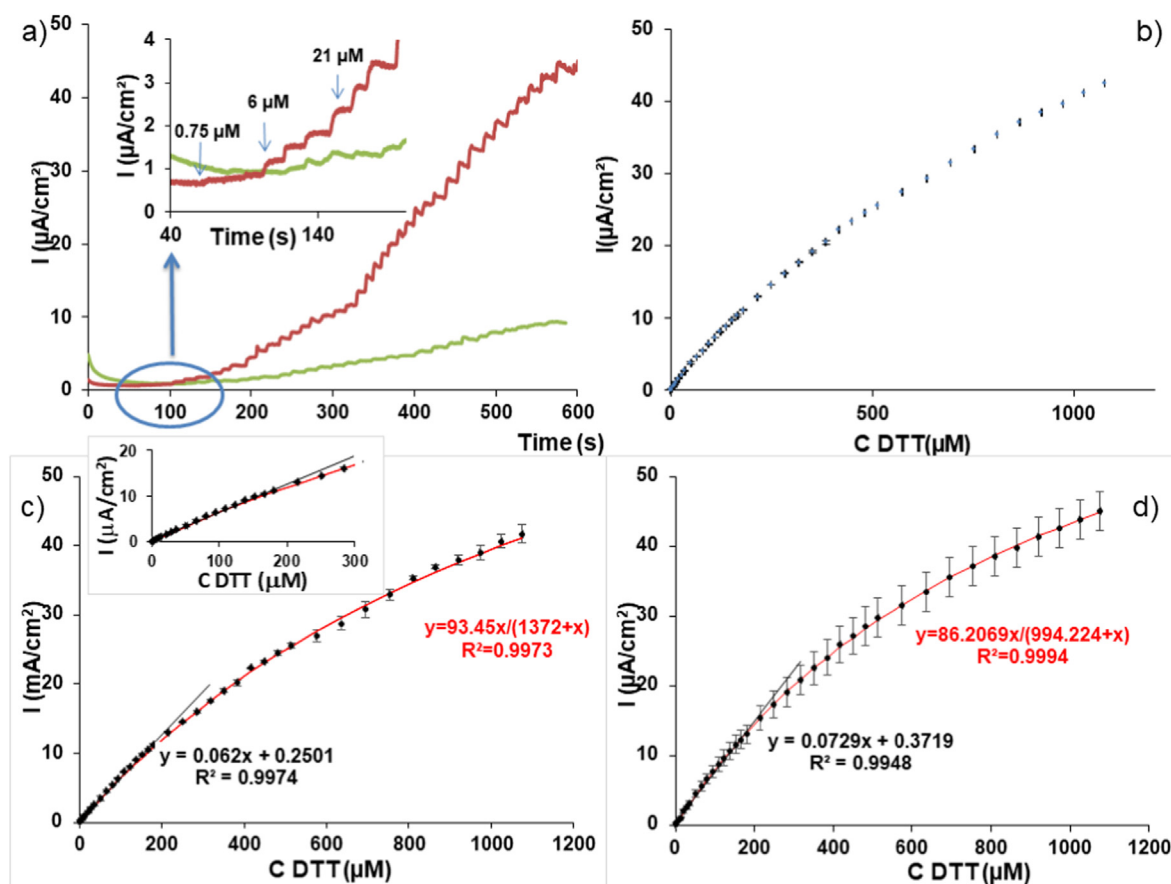
Fig. 5. (a) Amperometric response of GC/AuNPs (red trace), and bare GC (green trace) electrodes, towards DTT 0.750−1175 μM in stirred phosphate buffer (pH 7.4, I = 0.2) at +600 mV. A zoom of GC/AuNPs and bare GC responses to DTT 0.750, 6 and 21 μM is reported in the inset. (b) DTT calibration curve in 0.750−1175 μM concentration range on GC/AuNPs. (c) Typical fit of $I_{GC/AuNPs}$ vs DTT concentrations curve based on Langmuir isotherm obtained on the same GC/NPs electrode. Error bars represent one standard deviation about the mean obtained on the same GC/NPs electrode(n = 3). (d) Typical fit of $I_{GC/AuNPs}$ vs DTT concentration curve based on Langmuir isotherm averaged over three distinct GC/AuNPs sensors. Error bars represent one standard deviation about the mean obtained on three distints GC/NPs electrodes. (For interpretation of the references to colour in this figure legend, the reader is referred to the Web version of this article.)

considerably increasing the reactivity towards the DTT. In fact, a higher sensitivity is measured in comparison to bare GC. Also a very rapid time response below 2 s is typically observed. In detail, as reported in calibration curve (Fig. 5 (b)), it could be observed a dynamic range extended over 4 orders of magnitude. According to the Langmuir isotherm theory, the saturation of the response current is caused by the adsorption of DTT onto the catalyst surface. Therefore, based on the Langmuir isotherm theory, the equation $I = (a \times C_{DTT})/(b + C_{DTT})$ has been used to fit the calibration curves since electrochemical oxidation of DTT on the electrode is a surface catalytic reaction. The corresponding fitting equation ($R^2 = 0.9984$) for the GC/AuNPs electrode is presented as Eq. (6) which cover the broad dynamic range DTT detection of 0.750−1175 μM.

$$I_{CG/AuNPs} (\mu A cm^{-2}) = 93.46 \pm 0.06(\mu A\ cm^{-2})C_{DTT} (\mu M)/$$
$$(1372 \pm 6 + C_{DTT}) (\mu M) \qquad (6)$$

This trend has been further verified by linearizing the data reported as reciprocal,$1/I_{CG/AuNPs}$ and $1/C_{DTT}$, fitted with: $1/I=(b/a) \times (1/C_{DTT}) + (1/a)$, in the studied concentration range (data not shown). Moreover, the analysis confirmed that the dependence $I_{CG/AuNPs}$ vs C_{DTT} at low concentrations (i.e. 750 nM and 200 μM) can be traced back to a direct linear dependence as reported in Eq. (7).

$$I_{CG/AuNPs} (\mu A cm^{-2}) = 0.0620 \pm 0.0015(\mu A\ cm^{-2}\ \mu M^{-1})C_{DTT}$$
$$(\mu M) + 0.250 \pm 0.075 (\mu A cm^{-2}) \qquad (7)$$

The relevant determination coefficient is 0.9974. The reported repeatability of the sensor response is quantified as the RSD of the calibration slope (RSD_{slope}). These observations are in agreement with previous works regarding electro-catalysis of small molecules involved in processes at nano-structured electrodes [61−63]. The limit of DTT detection (LOD at a signal-to-noise ratio of 3) was measured being equal to 750 nM, a value that was almost three times smaller or better than that reported in similar previous works [23,43,64]. The influence of the amount of $AuCl_3$ (137 μM) aqueous solution on the sensor response has been evaluated and reported in the Supporting file (Fig. S5 (a) and (b)).

To test the suitability of the sensor to be applied in DTT detection to measure the oxidative potential of PM aqueous extracts, chrono-amperometric measurements were done to evaluate PM extracts potential interferences. The results are included and commented in Fig. S6 of the Supporting file.

3.5. Pulsed amperometric detection (PAD) of DTT whit SPE_GC/AuNPs sensor in FIA analysis

The Flow Injection analysis (FIA) presents many advantages compared with the batch analysis: the higher sample rates and the enhanced response time (often less than 30 s between sample injection and detection response). The required equipment is simple and more flexible and only a few microliters of sample volume are

M.P. Romano, M.G. Lionetto, A. Mangone et al.

necessary for the analysis, allowing the minimum reagent consumption. Thanks to these characteristics, FIA measurements are suitable for environmental analysis, especially when the number of samples is high and available sample volume is small or when on-line real-time measurements were requested. FIA measurements have been performed on SPE_GC/AuNPs electrodes. The critical parameters for the amperometric response in FIA analysis are the operating potential and the flow rate. The potential at +600 mV vs. SCE was selected as the potential value to be applied for the amperometric detection of DTT at the SPE_GC/AuNPs modified electrode, whit a flow rate of 1.5mLmin^{-1}, taking into account the compromise between the best signal to noise ratio and shorter analysis time. Pulsed amperometric detection (PAD) has been applied in order to reduce fouling of the electrode surface and avoid a loss of electroactivity over time. PAD measurement modality consists of 3 steps. The first, highly positive potential (+800 mV for 0.01s), caused oxide formation. The second potential, slightly negative (−1000 mV for 0.02 s), removed the oxide layer by reduction to reactivate the electrode. During the third step, the current was measured at the applied potential of +600 mV for 0.5 s. Typical FIA peaks for triplicate injections of different DTT concentration, between 10 and 500 μM, and relevant calibration curve is shown in Fig. 6. It could be observed a dynamic linear range extended over 2 orders of magnitude obtained by the regression analysis carried out with the following Eq. (6) with a determination coefficient of 0.998 in the concentration range between 10 μM and 500 μM.

$$I_{SPE\_GC/AuNPs} \ (\mu A cm^{-2}) = 0.0281(\mu A \ cm^{-2} \ \mu M^{-1})C_{DTT} \ (\mu M) - 0.043 \ (\mu A cm^{-2}) \ (6)$$

The repeatability of the method was evaluated by calculating the relative standard deviation for six injections of the DTT solutions at the same concentration for all 12 tested concentrations.

The stability of the amperometric response of the sensor has been tested by 72 successive injections of DTT 100 μM in phosphate buffer solution for about two and a half hours. Also interference studies have been performed to evaluate the effect of the PM aqueous extracts on DTT signals. Figures and related results are discussed in the Supporting (Fig.S7 and Fig.S8).

Relevant electroanalytical performances of the DTT sensors are reported in Table 1 that resumes and compares the analytical parameters of other similar and most significant electrochemical DTT sensors, based on (CoPCs)-modified carbon electrodes, with our results. It is important to note that the electro analytic performances of GC/AuNPs in terms of LOD, dynamic and linear ranges were always better than previous sensors class. In detail, the LOD is below 1 μM and the dynamic range can expand over 2-4 order of magnitude. In terms of sensitivity our sensor was less performing or comparable whit other sensors reported in Table 1, but however suitable to detect DTT decrement in OP measurements of PM aqueous extracts as obtained in reported validation tests with DTT spectroscopic assay reported below.

3.6. FIA analysis of DTT rate consumption in PM aqueous extracts

In order to test the suitability of the electrochemical DTT assay for measuring the OP in real samples, we have reported some preliminary FIA experiments addressed to measure the DTT (100 μM) rate consumption, $\delta_{DTT-Electrochemical}$ activity, in PM$_{10}$ aqueous extracts. Moreover, with the aim to validate the method, obtained results were compared with data obtained on the same
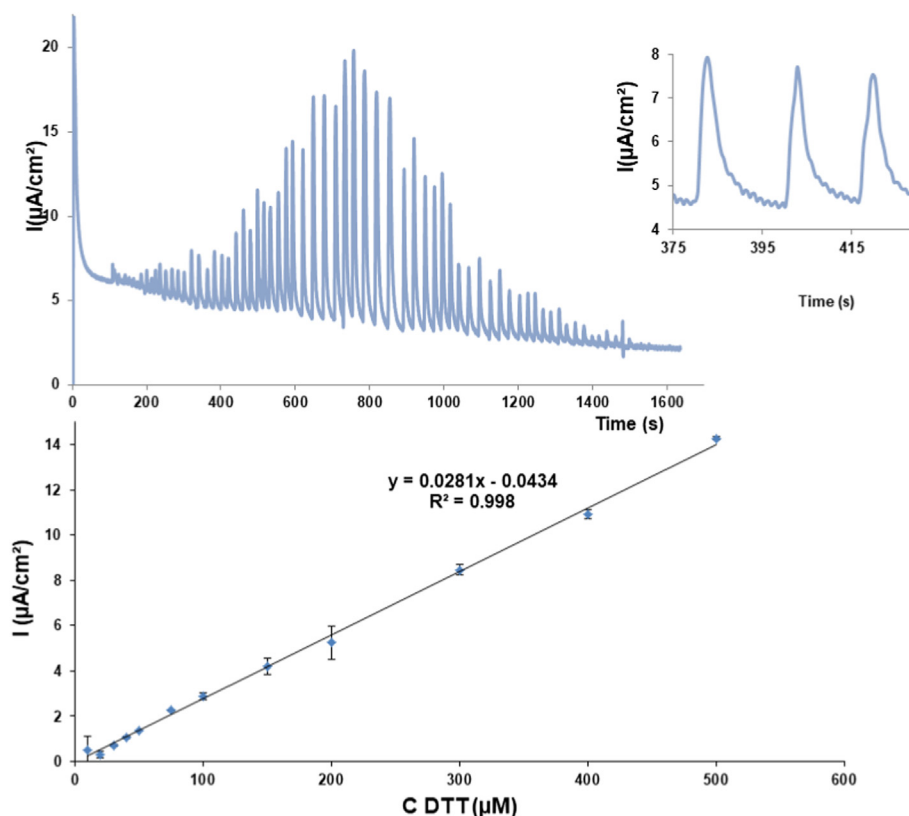
Fig. 6. PAD experiments in FIA analysis. (a) Peaks recorded for six injections of DTT and inset with peaks for injections of DTT 100 μM (b) relevant calibration curve. Carrier: phosphate buffer solution (pH = 7.4, I = 0.2); flow rate: 1.5 mL min^{-1}.

Table 1

Comparison between the analytical performances of GC/AuNPs and SPE_GC_NPs and other similar DTT electrochemical sensors reported in the literature. For completeness also a spectrophotometric method has been added. °DropSens 410 SPE. *Polycaprolactone. ^Peak Area/[CDTT](mAU*min/μM).

Methods	Sensor	Dynamic range (μM)	Linear range (μM)	LOD (μM)	Sensitivity (nA/μM)	References
Amperometric (microfluidic)	CoPC-CPEs	Not provided	<100	2.50	Not provided	[43]
Amperometric (microfluidic)	CoPC−CPE	10−100	10−100	2.40	37	[23]
Amperometric (FIA)	CoPC-Carbon°	25−100	25−100	8.45	13.7	[64]
Amperometric (HPLC)	Graphite-CoPC-PCL*	<115	<115	-	10	[26]
Amperometric (HPLC)	CoPC-Carbon°	<110	<110	-	6−27	[26]
Spectrophotometric (HPLC)	-	<100	<100	-	0.150^	[26]
Amperometric (BIA)	CG-AuNPs	0.750−1175	0.750−200	0.750	5	This work
Amperometric (FIA)	SPE_CG-AuNPs	10−500	10−500	1.5	2	This work

PM samples using the traditional spectrophotometric method based on the Ellman's reactive use (DTT assay) [31], assumed as a recognized reference method [64]. A total of six samples, representative of different PM sources, were then tested in parallel with both methods. Related experimental details and methods to measure the δ_{DTT} activity, defined as the DTT rate consumption in pmol/min, and the OP_{DTT-M} normalized for the PM mass (μg), are reported in the supporting file and summarized in Table S1. As a usual procedure, before PM samples analysis, the method has been tested by calibrating the electroanalytical sensor in PQN standard solutions (i.e., 0.025 and 0.050 μM) used as a PM model oxidant of DTT (100 μM). In this case, the δ_{DTT-M} activity has been normalized to respect PQN mass in μg. A typical linear regression obtained by measuring the peak currents density decrement versus time in presence of PQN 0.025 μM is reported in Fig. S9. The linearity is observed in a time range of 60 min for both PQN 0.050 and 0.025 μM. The related measured δ_{DTT} activity are 66.6 and 63.2 nmoli/min for μg of PQN, respectively for PQN 0.025 and PQN 0.050 μM. The PQN test is used as a positive controls before using the sensor in the analysis of PM extracts [64]. In Fig. S10 (a) a typical electrochemical FIA experiment recorded to detect DTT activity in a PM aqueous extract (Filter 9) is reported. A decrement of DTT peak signals is observed during the reaction time of 90 min. The relevant curve obtained reporting the peak currents recorded at different reaction time: 5, 10, 15, 20, 30, 40, 60 and 90 min is shown in Fig. S10 (b). The linear slope and intercept in the time range of 60−90 min has been obtained for all six samples and used to calculate $OP_{DTT-M\_Electrochemical}$ activity in pmoli/min*μg of PM. In Fig. S10 (c) the related measurements of DTT absorbance in spectrophotometric method obtained in parallel on the same samples, picked-up during the reaction time, has been also reported to validate the method by measuring the $OP_{DTT-UV-vis}$ (pmoli/min*μg) (experimental details in supporting file). In Fig. S11 the $OP_{DTT-Electrochemical}$ (pmoli/min*μg) activities were compared with $OP_{DTT-UV-vis}$ (pmoli/min*μg) data, obtained in parallel on the same samples. As evident the OP_{DTT-M} values obtained whit both methods are coherent and in accordance with averaged data reported in the area of monitoring [34]. The observed variability of the results between the two methods is in line with the level of the RSDs of both.

4. Conclusions

In this paper, an electrochemical sensor based on GC modified with electrodeposited gold nanoparticles, suitable for the measurement of oxidative potential of atmospheric particulate matter, has been developed and characterized. The proof of the concept was to propose the new sensor as an alternative to the classic spectrophotometric DDT assay method. The operating principle is the measurement of the loss in DTT content in the reduced form, exploiting its electro-active properties in oxidation.

The modified electrodes obtained by the electrochemical deposition of gold nanoparticles on glassy carbon electrodes have been chemically and morphologically characterized by XPS and SEM/EDS analysis. The electrochemical properties have been evaluated by CV and CA measurements in phosphate buffer, in the absence and in presence of DTT, respectively. The electrochemical sensor performances are considerably influenced by the nanoparticles, which were optimized to yield a stable and reproducible response to respect DTT detection.

All the experiments to test the electroanalytical performances of the sensor have been carried out in Batch and Flow Injection Analysis at an operative potential of +600 mV, where the interference of real PM aqueous extract in the electrochemical response to DTT was negligible in analytical terms confirming the high selectivity of the method.

Moreover, data collected from these experiments show that the electroanalytical performances of the tested sensors make them suitable for the quantitative determination of DTT substrates in terms of high sensitivity (0.0622 μA cm^{-2} μM^{-1} and 0.0281 μA cm^{-2} μM^{-1}), low detection limit (0.750 μM and 1.5 μM), wide linear and dynamic ranges extended over 2-4 orders of magnitude, response time (few s) and reproducibility of the method. Finally, the proposed method has been used in the measurements of OP for six PM real samples and validated by using the classic spectrophotometric method. All these results together with the absence of interference of real PM aqueous extract in the electrochemical response to DTT make the sensor suitable to be applied in oxidative potential measurements of particulate atmosphere oxidative potential.

CRediT authorship contribution statement

Maria Pia Romano: Conceptualization, Methodology, Investigation, Writing − original draft, All authors collaborated to interpretation of results, read, commented, and approved the final manuscript. **Maria Giulia Lionetto:** Visualization, Writing − original draft, Supervision, All authors collaborated to interpretation of results, read, commented, and approved the final manuscript. **Annarosa Mangone:** Visualization, Investigation, All authors collaborated to interpretation of results, read, commented, and approved the final manuscript. **Anna Rita De Bartolomeo:** Investigation, All authors collaborated to interpretation of results, read, commented, and approved the final manuscript. **Maria Elena Giordano:** Investigation, All authors collaborated to interpretation of results, read, commented, and approved the final manuscript. **Daniele Contini:** Resources, Writing − original draft, Supervision, All authors collaborated to interpretation of results, read, commented, and approved the final manuscript. **Maria Rachele Guascito:** Conceptualization, Writing − original draft, Supervision, Writing − review & editing, All authors collaborated to interpretation of results, read, commented, and approved the final manuscript.

M.P. Romano, M.G. Lionetto, A. Mangone et al.

Declaration of competing interest

The authors declare that they have no known competing financial interests or personal relationships that could have appeared to influence the work reported in this paper.

Acknowledgements and funding

Appendix A. Supplementary data

Supplementary data to this article can be found online at https://doi.org/10.1016/j.aca.2022.339556.

References

[1] C.E. Hand, J.F. Honek, Biological chemistry of naturally occurring thiols of microbial and marine origin, J. Nat. Prod. 68 (2005) 293, https://doi.org/10.1021/np049685x.

[2] W.A. Kleinman, J.P. Richie Jr., Status of glutathione and other thiols and disulfides in human plasma, Biochem. Pharmacol. 60 (Issue 1) (2000) 19–29, https://doi.org/10.1016/S0006-2952(00)00293-8.

[3] M. Valko, D. Leibfritz, J. Moncol, M.T. Cronin, M. Mazur, J. Telser, Free radicals and antioxidants in normal physiological functions and human disease, Int. J. Biochem. Cell Biol. 39 (2007) 44.

[4] L. Rojas, L. Molero, R.A. Tapia, R. del Rio, M.A. del Valle, M. Antilén, F. Armijo, Electrochemistry behavior of endogenous thiols on fluorine doped tin oxide electrodes, Electrochim. Acta 56 (Issue 24) (2011) 8711–8717, https://doi.org/10.1016/j.electacta.2011.07.074.

[5] D.A. Dickinson, H.J. Forman, Cellular glutathione and thiols metabolism, Biochem. Pharmacol. 64 (5–6) (2002) 1019–1026, https://doi.org/10.1016/S0006-2952(02)01172-3.

[6] J.R. Winther, C. Thorpe, Quantification of thiols and disulfides, Biochim. Biophys. Acta (BBA) 2014-Gen. Subj. (2) (1840) 838–846.

[7] G.L. Ellman, Tissue sulphydil groups, Arch. Biochem. Biophys. 82 (1959) (1959) 70–77.

[8] J.C. Harfield, C. Batchelor-McAuley, R.G. Compton, Electrochemical determination of glutathione: a review, Analyst 137 (2012) 2285–2296.

[9] H. Konno, H. Yasumiishi, A. Roki, I. Nitanai, S. Yano, Detection of thiol functionality and disulfide bond formation by polyoxometalate, ACS Comb. Sci. 22 (12) (2020) 745–749.

[10] P.C. White, N.S. Lawrence, J. Davis, R.G. Compton, Electrochemical determination of thiols: a perspective, Electroanalysis (2002), https://doi.org/10.1002/1521-4109(200201)14:2<89::AID-ELAN89>3.0.CO;2-Y.

[11] N.F. Atta, A. Galal, S.M. Azab, Novel sensor based on carbon paste/Nafion® modified with gold nanoparticles for the determination of glutathione, Anal. Bioanal. Chem. 404 (2012) 1661–1672, https://doi.org/10.1007/s00216-012-6276-0, 2012.

[12] S.A. Zaidi, J.H.A. Shin, A review on the latest developments in nanostructure-based electrochemical sensors for glutathione, Anal. Methods 8 (2016) 1745.

[13] A. Hamad, M. Elshahawy, A. Negm, F.R. Mansour, Analytical methods for determination of glutathione and glutathione disulfide in pharmaceuticals and biological fluids, Rev. Anal. Chem. 38 (2020) 1–32.

[14] J.L. D' Eramo, A.E. Finkelstein, F.O. Boccazzi, O. Fridman, Total homocysteine levels in plasma: high-performance liquid chromatographic determination with electrochemical detection and glassy carbon electrode, J. Chromatogr. 720 (1998) 205.

[15] I.B. Santarino, S.C.B. Oliveira, A.M. Oliveira-Brett, Protein reducing agents dithiothreitol and tris(2-carboxyethyl)phosphine anodic oxidation, Electrochem. Commun. (2012) 114–117.

[16] A. Wang, L. Zhang, S. Fang, Y. Zhang, Determination of thiols following their separation by CZE with amperometric detection at a carbon electrode, J. Pharm. Biomed. Anal. 23 (2000) 429.

[17] R. Gogia, S.P. Richer, R.C. Rose, Tear fluid content of electrochemically active components including water soluble antioxidants, Curr. Eye Res. 17 (1998) 257.

[18] G.S. Owens, W.R. La Course, Pulsed electrochemical detection of thiols and disulfides following capillary electrophoresis, J. Chromatogr. B 695 (1997) 15.

[19] T.S. Jovanovic, B.S. Stanovic, Silver and platimun electrodes in the direct potentiometric determination of N-acetyl-L-Cysteine with copper acta pharm, Jugoslavica 39 (1989) 117.

[20] K.M. Korfhage, K. Ravichandran, R.P. Baldwin, Phthalocyanine-containing chemically modified electrodes for electrochemical detection in liquid chromatography/flow injection systems, Anal. Chem. 56 (1984) 1514.

[21] M.K. Halbert, R.P. Baldwin, Electrocatalytic and analytical response of cobalt phthalocyanine containing carbon paste electrodes toward sulfhydryl compounds, Anal. Chem. 57 (1985) 591.

[22] N. Pereira-Rodrigues, R. Cofre, J.H. Zagal, F. Bedioui, Electrocatalytic activity of cobalt phthalocyanine CoPc adsorbed on a graphite electrode for the oxidation of reduced l-glutathione and reduction of its disulfide (GSSG) at physiological pH, Bioelectrochemistry 70 (2007) 147–154.

[23] Y. Sameenoi, K. Koehler, J. Shapiro, K. Boonsong, Y. Sun, J. Collett Jr., J. Volckens, C.S. Henry, Microfluidic electrochemical sensor for on-line monitoring of aerosol oxidative activity, J. Am. Chem. Soc. 134 (25) (2012) 10562–10568, 2012.

[24] K. Koehler, J. Shapiro, Y. Sameenoi, C. Henry, J. Volckens, Laboratory evaluation of a microfluidic electrochemical sensor for aerosol oxidative load, Aerosol. Sci. Technol. 48 (2014) 489–497, https://doi.org/10.1080/02786826.2014.891722.

[25] P.K. Sarswat, L. Free, Real-time detection of thiols using CoPc modified black-phosphorus based sensors, J. Electrochem. Soc. 166 (2) (2019) B1. B1-B8.

[26] K.E. Berg, K.M. Clark, X. Li, M. Ellison, E.M. Carter, J. Volckens, C.S. Henry, High-throughput, semi-automated dithiothreitol (DTT) assays for oxidative potential of fine particulate matter, Atmos. Environ. 222 (1) (2020) 117132.

[27] M. Scampicchio, N.S. Lawrence, A. Arecchi, S. Mannino, Electrochemical reduction of Ellman's reagent: a novel selective detection protocol for thiol compounds, Eletroanalysis 19 (23) (2007).

[28] W.W. Cleland, Dithiothreitol, a new protective reagent for SH groups, Biochemistry 3 (1964) 480–482.

[29] G.T. Hermanson, Functional targets for bioconjugation, in: Bioconjugate Techniques, third ed., Academic Press, Boston, MA, USA, 2013, pp. 127–228.

[30] Y. Kumagai, S. Koide, K. Taguchi, A. Endo, Y. Nakai, T. Yoshikawa, N. Shimojo, Oxidation of proximal protein sulfhydryls by phenanthraquinone, a component of diesel exhaust particles, Chem. Res. Toxicol. 15 (4) (2002) 483–489, https://doi.org/10.1021/tx01009939.

[31] A.K. Cho, C. Sioutasa, A.H. Miguela, Y. Kumagaia, D.A. Schmitza, M. Singha, A. Eiguren-Fernandeza, J.R. Froines, Redox activity of airborne particulate matter at different sites in the Los Angeles Basin Environmental, Research 99 (2005) 40–47.

[32] J.O. Anderson, J.G. Thundiyil, A. Stolbach, Clearing the air: a review of the effects of particulate matter air pollution on human health, JMT 8 (2012) 166–175.

[33] S. Liu, Y. Zhou, S. Liu, X. Chen, W. Zou, D. Zhao, X. Li, J. Pu, L. Huang, J. Chen, et al., Association between exposure to ambient particulate matter and chronic obstructive pulmonary disease: results from a cross-sectional study in China, Thorax 72 (2017) 788–795.

[34] M.G. Lionetto, M.R. Guascito, M.E. Giordano, R. Caricato, A.R. De Bartolomeo, M.R. Romano, M. Conte, A. Dinoi, D. Contini, Oxidative Potential, cytotoxicity, and intracellular Oxidative Stress generating capacity of PM10: a case study in South of Italy, Atmosphere 12 (2021) 464, https://doi.org/10.3390/atmos12040464.

[35] Y. Kumagai, Y. Abiko, N.L. Cong, Chemical toxicology of reactive species in the atmosphere: two decades of progress in an electron acceptor and an electrophile, J. Toxicol. Sci. 41 (2016) SP37–SP47, https://doi.org/10.2131/jts.41.SP37.

[36] J.T. Bates, T. Fang, V. Verma, L. Zeng, R.J. Weber, P.E. Tolbert, J.Y. Abrams, S.E. Sarnat, M. Klein, J.A. Mulholland, et al., Review of acellular assays of ambient particulate matter oxidative potential: methods and relationships with composition, sources, and health effects, Environ. Sci. Technol. 53 (2019) 4003–4019.

[37] R. Weber, T. Fang, V. Verma, Insights on aerosol oxidative potential from measurements of particle size distributions, in: Multiphase Environmental Chemistry in the Atmosphere, vol. 1299, American Chemical Society, Washington, DC, USA, 2018, pp. 417–437.

[38] H. Jiang, C.M. Sabbir Ahmed, A. Canchola, J.Y. Chen, Y. Jin Chen, Y.H. Lin, Use of Dithiothreitol Assay to Evaluate the Oxidative Potential of Atmospheric Aerosols, Review, Atmosphere, 2019.

[39] H. Guo, L. Lei Jin, S. Huang, Effect of PM characterization on PM oxidative potential by acellular assays: a review, Rev. Environ. Health 35 (4) (2020) 461–470.

[40] M.C. Pietrogrande, M. Russo, E. Zagatti, Review of PM oxidative potential measured with acellular assays in urban and rural sites across Italy, Atmosphere 10 (10) (2019) 626, https://doi.org/10.3390/atmos10100626.

[41] D. Chirizzi, D. Cesari, M.R. Guascito, A. Dinoi, L. Giotta, A. Donateo, D. Contini, Influence of Saharan dust outbreaks and carbon content on oxidative potential of water-soluble fractions of PM2.5 and PM10, Atmos. Environ. 163 (2017) 1–8.

[42] T. Fang, V. Verma, H. Guo, L.E. King, E.S. Edgerton, R.J. Weber, A semi-automated system for quantifying the oxidative potential of ambient particles in aqueous extracts using the dithiothreitol (DTT) assay: results from the Southeastern Center for Air Pollution and Epidemiology (SCAPE), Atmos. Meas. Tech. 8 (2015) 471–482.

[43] Y. Sameenoi, M.M. Mensack, K. Boonsong, R. Ewing, Wijitar Dungchai, Orawan Chailapakul, Donald M. Cropeke, S. Charles, Henry **Poly(dimethylsiloxane) cross-linked carbon paste electrodes for microfluidic electrochemical sensing**, Analyst 136 (2011) 3177–3184.

[44] L. Agüí, L, C, C. Peña-Farfal, P. Yáñez-Sedeño, J.M. Pingarrón, Electrochemical determination of homocysteine at a gold nanoparticle-modified electrode,

Talanta 74 (2007) 412—420.

[45] J. Xie, D. Cheng, P. Li, Z. Xu, X. Zhu, Y. Zhang, H. Li, X. Liu, M. Liu, S. Yao, Au/Metal—Organic framework nanocapsules for electrochemical determination of glutathione, ACS Appl. Nano Mater. (2021), https://doi.org/10.1021/acsanm.1c00394. XXXX, XXX.

[46] K.E. Berg, L.R. Turner, M.L. Benka-Coker, S. Rajkumar, B.N. Young, J.L. Peel, M.L. Clark, J. Volckens, C.S. Henry, Electrochemical dithiothreitol assay for large-scale particulate matter studies, Aerosol. Sci. Technol. 53 (3) (2019) 268—275.

[47] S. Alim, J. Vejayan, M.M. Yusoff, A.K.M. Kafi, Recent uses of carbon nanotubes & gold nanoparticles in electrochemistry with application in biosensing: a review, Biosens. Bioelectron. 121 (2018) 125—136.

[48] S.K. Guin, J.S. Pillai, A.S. Ambolikar, A. Saha, S.K. Aggarwal, Template-free electrosynthesis of gold nanoparticles of controlled size dispersion for the determination of lead at ultratrace levels, RSC Adv. 3 (2013), 17977—17988 | 17977.

[49] T. Hezard, K. Fajerwerg, D. Evrard, V. Colliere, P. Behra, P. Gros, Gold nanoparticles electrodeposited on glassy carbon using cyclic voltammetry: application to Hg(II) trace analysis, J. Electroanal. Chem. 664 (1) (2012) 46—52.

[50] M. Conte, E. Merico, D. Cesari, A. Dinoi, F.M. Grasso, A. Donateo, M.R. Guascito, D. Contini, Long-term characterisation of African dust advection in southeastern Italy: influence on fine and coarse particle concentrations, size distributions, and carbon content, Atmos. Res. 233 (2020) 104690.

[51] D. Cesari, G.E. De Benedetto, P. Bonasoni, M. Busetto, A. Dinoi, E. Merico, D. Chirizzi, P. Cristofanelli, A. Donateo, F.M. Grasso, A. Marinoni, A. Pennetta, D. Contini, Seasonal variability of PM2.5 and PM10 composition and sources in an urban background site in Southern Italy, Sci. Total Environ. 612 (2017) 202—213.

[52] M.R. Guascito, G. Ricciardi, A. Rosa, Nickel-macrocycle interaction in nickel(II) porphyrins and porphyrazines bearing alkylthio β-substituents: a combined DFT and XPS study, J. Porphyr. Phthalocyanines 21 (2017) 371—380.

[53] J.E. Castle, A.M. Salvi, Interpretation of the Shirley background in x-ray photoelectron spectroscopy analysis, J. Vacuum Sci. Technol. A Vacuum Surf. Films 19 (4) (2001) 1170—1175, https://doi.org/10.1116/1.1378074.

[54] J.R. Waldrop, R.W. Grant, Y.C. Wang, R.F. Davis, Metal Schottky barrier contacts to alpha 6H-SiC, J. Appl. Phys. 72 (1990) 4757.

[55] T. Bhuvana, G.V. Pavan Kumar, Chandrabhas Narayana, G.U. Kulkarni, Nanogranular Au films deposited on carbon covered Si substrates for enhanced optical reflectivity and Raman scattering, Nanotechnology 18 (2007) 7, https://doi.org/10.1088/0957-4484/18/14/145702, 145702.

[56] W.R. LaCourse, G.S. Owens, Pulsed electrochemical detection of thiocompounds following microchromatographic separations, Anal. Chim. Acta 307 (1995) 301.

[57] D.C. Johnson, W.R. LaCourse, Liquid chromatography with pulsed electrochemical detection at gold and platinum electrodes, Anal. Chem. 62 (10) (1990) 589A—597A.

[58] J.B. Schlenoff, J, B, M. Li, M. H, H. Ly, Stability and self-exchange in alkanethiol monolayers, J. Am. Chem. Soc. 117 (1995) 12528—12536.

[59] A. Ulman, Formation and structure of self-assembled monolayers, Chem. Rev. 96 (1996) 1533—1554.

[60] B. Svensmark, O. Hammerich, H. Lund, M.M. Baizer (Eds.), Organic Electrochemistry. An Introduction and a Guide, Marcel Dekker, NY, 1991, p. 660.

[61] D. Thirumalai, D. Subramani, B. Shin, H.-J. Paik, S.-C Chang, A metal-free, nonenzymatic electrochemical glucose sensor with a de-bundled single-walled carbon nanotube-modified electrode, Bull. Kor. Chem. Soc. 39 (2018) 141—145.

[62] R. Liang, A. Hu, J. Persic, Y.N. Zhou, Palladium nanoparticles loaded on carbon modified TiO2 nanobelts for enhanced methanol electrooxidation, Nano-Micro Lett. 5 (2013) 202—212.

[63] E. Filippo, F. Baldassarre, M. Tepore, M. R. Guascito, D. Chirizzi, A. Tepore. Characterization of hierarchical α-MoO3 plates toward resistive heating synthesis: electrochemical activity of α-MoO3/Pt modified electrode toward methanol oxidation at neutral pH. Nanotechnology, Volume 28, Number 21.

[64] K.E. Berg, L.R. Turner, M.L. Benka-Coker, S. Rajkumar, B.N. Young, J.L. Peel, M.L. Clark, J. Volckens, C.S. Henry, Electrochemical dithiothreitol assay for large-scale particulate matter studies, Aerosol. Sci. Technol. 53 (3) (2019) 268—275.